

Search for Charginos and Neutralinos in R-Parity Violating Scenario with $\lambda' LQD$ Couplings at $\sqrt{s} = 189$ GeV

C. Mulet-Marquis

Institut des Sciences Nucléaires de Grenoble

Abstract

Neutralino and chargino pair production at $\sqrt{s} = 189$ GeV are studied in R-parity violating scenario with a dominant LQD (λ') coupling leading to two jets and a neutrino or a muon in the final state of the $\tilde{\chi}_1^0$ R_p violating decay. This study covers the λ'_{i3k} ($i = 1, 3, k = 1, 2, 3$) and λ'_{2jk} ($j = 1, 2, k = 1, 2, 3$) couplings. The aim of the work is to update the analyses presented in the reference [1]. No deviation from standard model is observed. The results are used to exclude domains of the Minimal Supersymmetric Standard Model parameter space and to derive a lower limit on neutralino and chargino mass. The limits are $30 \text{ GeV}/c^2$ for $\tilde{\chi}_1^0$ and $94 \text{ GeV}/c^2$ for $\tilde{\chi}_1^+$.

1 Introduction

The Minimal Supersymmetric Standard Model (MSSM) [2] is the minimal extension of the Standard Model (SM) in terms of the number of particles. To each SM particle is associated a supersymmetric partner (called Sparticle in the following), whose spin differs by 1/2, and an extra $SU(2)_L$ Higgs doublet is added. One can define the R_p quantum number as $R_p = (-1)^{3B+L+2S}$ where B, L, and S are respectively the baryon number, lepton number and spin. For SM particles $R_p = +1$ and for their supersymmetric partner $R_p = -1$. The most general supersymmetric Lagrangian involves the R-parity violating terms [3] $\lambda_{ijk} L_i L_j \bar{E}_k + \lambda'_{ijk} L_i Q_j \bar{D}_k + \lambda''_{ijk} \bar{U}_i \bar{D}_j \bar{D}_k$ where λ_{ijk} , λ'_{ijk} and λ''_{ijk} are Yukawa couplings, L and E (Q, U and D) denote the lepton (quark) superfields.

The main consequence of the R-parity violation, R_p is that the Lightest Supersymmetric Particle (LSP) is no more stable and can decay into SM particles. The decay of a Sparticle can be either *direct*, when the Sparticle decays directly or via a virtual exchange of a squark or a slepton to standard particle through an R_p vertex (this is always the case for the LSP), or *indirect* when the Sparticle first decays through an R_p conserving vertex to a standard particle and an on-shell Sparticle which then decays through an R_p vertex. Figure 1 shows the R_p decays of squarks and sleptons with λ' couplings, figure 2 illustrates the $\tilde{\chi}_1^0$ three body direct decay in a lepton (charged or neutral) and 2 quarks (the flavour of the lepton depends of the index i and those of the quarks of the indices j and k) and the $\tilde{\chi}_1^+$ indirect decay in a W^* and a $\tilde{\chi}_1^0$.

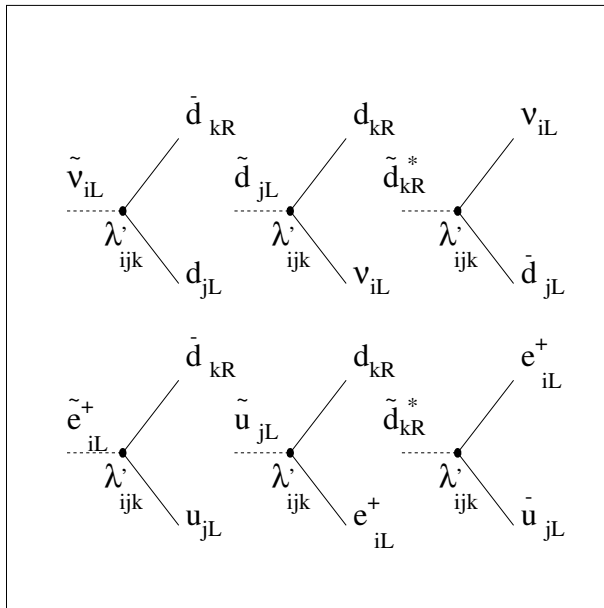


Figure 1: R_p decays of sfermions with λ' couplings.

2 Framework of the analysis

This paper presents an update at 189 GeV of the results presented in [1] concerning the search for $\tilde{\chi}_1^0$ and $\tilde{\chi}_1^+$. Because the luminosity was in 1998 three times larger in 1997,

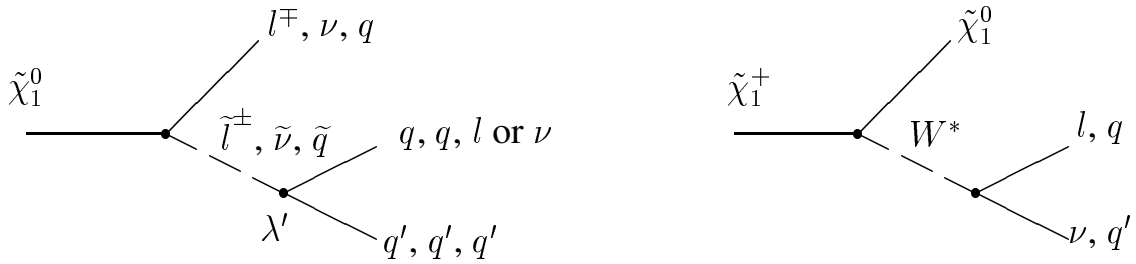


Figure 2: $\tilde{\chi}_1^0$ direct decay with λ' couplings (left) and $\tilde{\chi}_1^+$ indirect decay(right).

an efficient method of discrimination between background and signal was needed in some analyses. A Fisher discriminant method [14] was used to further reduce the background in the case of the neutralino decaying in a neutrino and two quarks. A sequential analysis is made for the case of the neutralino decaying in a muon and two quarks. When the λ'_{ijk} couplings involve b quarks in the three body decay of the neutralino, the AABTAG [4] package was used for the b -tagging. This algorithm combines informations from impact parameters and rapidities of the tracks to build a probability which is close to 1 if the event does not contain a b quark, and is near 0 if the event has a high b content. The probability variables of tagging P_E (obtained with all tracks) and P_E^+ (obtained with tracks having a positive impact parameter, i.e. the vector joining the primary vertex and the point of closest approach of the track is in the same direction that the jet to which the track belongs) are defined in [4] and [5]. Jets are reconstructed using the Durham algorithm.

For the λ'_{ijk} couplings, with $i = 1, 2, 3$, $j = 1, 2$, $k = 1, 2, 3$, the two decays

- $\tilde{\chi}_1^0 \rightarrow l_i qq$
- $\tilde{\chi}_1^0 \rightarrow \nu_i qq$

are allowed. In this paper, only the muon channel is studied when the $\tilde{\chi}_1^0$ decays into a charged lepton (and two quarks).

For the λ'_{i3k} , $i = 1, 2, 3$, $k = 1, 2, 3$ couplings only the decay

- $\tilde{\chi}_1^0 \rightarrow \nu_i bq$, $q \neq b$ or $q = b$

is allowed at LEP. Indeed, in the three-body decay of the $\tilde{\chi}_1^0$ the charged lepton would be produced with a top quark, according to the R-parity violating term $\lambda'_{ijk} L_i Q_j \bar{D}_k$ of the MSSM Lagrangian [3]. This requires neutralinos with masses greater than the top quark mass. Since the neutralinos would be produced by pairs at LEP the channel $\tilde{\chi}_1^0 \rightarrow e_i t q$ is not opened.

The common value for the λ' to generate signal events is set to 0.01 which is below the indirect limits obtained from SM processes on the couplings except for λ'_{111} and λ'_{133} . In that particular case the low energy measurements impose $\lambda'_{111} \leq 5.2 \cdot 10^{-4}$ [6] and $\lambda'_{133} \leq 1.4 \cdot 10^{-3}$ [7]. As a consequence, the length of flight of $\tilde{\chi}_1^0$ is non negligible (from a few tenth of centimeter to a few meters) in restricted regions of $\mu - M_2$ plane : the present analyses are not sensitive to such cases of displaced vertices.

3 Data samples

The data corresponding to an integrated luminosity of 158 pb^{-1} collected during 1998 by DELPHI at center of mass energy of 189 GeV were analysed.

Concerning the background different contributions coming from Standard Model processes : Bhabha scattering, $e^+e^- \rightarrow Z\gamma, \gamma\gamma$, 4 fermions final states were considered. $Z\gamma \rightarrow \text{hadrons}, \tau^+\tau^-, \mu^+\mu^-$ were produced by PYTHIA[8] and KORALZ[9]. The $\gamma\gamma$ samples used were produced at 184 GeV. $\gamma\gamma$ interactions leading to leptonic final states were generated with the BDK program [10]; the $\gamma\gamma \rightarrow \text{hadrons}$ were generated using TWOAM[11]. The four fermions final states were studied with EXCALIBUR[12].

To evaluate signal efficiencies, neutralino and chargino pair production were generated with SUSYGEN 2.20.3[13]. Several points in the MSSM parameter space, corresponding to different values of $\tan\beta$ (1.01, 1.5, 5 and 30), m_0 (90, 300 and 500 GeV/ c^2), μ ($-300 \leq \mu \leq 300$ GeV/ c^2) and M_2 ($0 < M_2 \leq 400$ GeV/ c^2) were considered. All generated signal events were processed with the DELPHI full simulation program.

4 Case $\tilde{\chi}_1^0 \rightarrow \nu_i qq$

When there is at least one b quark in the decay of the $\tilde{\chi}_1^0$, i.e for λ'_{i3k} , $i = 1, 2, 3$, $k = 1, 2, 3$, or λ'_{ij3} , $i = 1, 2, 3$, $j = 1, 2$, the study was made considering both $e^+e^- \rightarrow \tilde{\chi}_1^0\tilde{\chi}_1^0$ (with a direct decay of the $\tilde{\chi}_1^0$) and $e^+e^- \rightarrow \tilde{\chi}_1^+\tilde{\chi}_1^-$ (with an indirect decay of the $\tilde{\chi}_1^+$ as shown in figure 2 and the direct decay $\tilde{\chi}_1^0 \rightarrow \nu_i qq$). For the other λ'_{ijk} couplings considered in this note (no b quark in the decay of the $\tilde{\chi}_1^0$), the channel $\tilde{\chi}_1^0 \rightarrow \nu_i qq$ is most efficiently covered with $e^+e^- \rightarrow \tilde{\chi}_1^+\tilde{\chi}_1^-$ (with an indirect decay of the $\tilde{\chi}_1^+$). Of course the analyses are not sensitive to the flavor of the neutrino, that is to say to the value of the i index.

4.1 Indirect decay of the charginos

A set of general preselection cuts are made before applying the Fisher discriminant analysis. These criteria are in common for all the analyses, that is to say do not suppose the presence or not of a b quark. They are based on very general characteristics of the signal as can be seen in table 1 : the charged multiplicity of the event and its charged energy, missing quantities (invisible mass, $Pt_{miss}, |\cos(\theta_{miss})|$) related to the two neutrinos in the $\tilde{\chi}_1^0$ decay, and topological variables (the thrust, the minimum angle between jets when the event is forced into a four-jet event, and the number of reconstructed jets with a Durham Y_{cut} of 0.0024). The number of remaining real events and Monte-Carlo events are reported in table 1.

The 95 % confidence level is calculated according the Feldman and Cousins prescription [15]. The content of the Fisher variable in each case is described in table 2. Y_6 is the Durham distance at which the event topology flips from 5 to 6 jets.

4.2 Direct decay of the neutralinos

As said above, only the case of the $\tilde{\chi}_1^0$ decaying into a neutrino and at least one b quark is considered. As for the $\tilde{\chi}_1^+$ case a set of preselection criteria is applied before using a Fisher analysis. They are namely : the charged multiplicity of the event and its charged energy, the missing quantities (invisible mass, $Pt_{miss}, |\cos(\theta_{miss})|$) related to the two neutrinos

Step	Selection criteria	Data	Background	Efficiency
1	Charged multiplicity ≥ 10 $E_{char} \geq 35$ GeV Invisible Mass ≥ 20 GeV $Pt_{miss} \geq 5$ GeV/c $ \cos(\theta_{miss}) \leq 0.9$	4327	4410 \pm 14.7	84
2	Thrust ≤ 0.93	2976	3006 \pm 12.1	84
3	Minimum angle between 4 jets $\geq 20^\circ$	2143	2198.5 \pm 10.7	83
4	More than 6 jets for $Y_c=0.0024$	513	503.8 \pm 5.5	74
5	Fisher Variable $u \geq$ -0.7 (λ'_{ijk} , $i = 1, 2, 3$, $j, k = 1, 2$) 0 (λ'_{i3k} , $i = 1, 2, 3$, $k = 1, 2$) λ'_{ij3} , $i = 1, 2, 3$, $j = 1, 2$ -0.65 (λ'_{i33} , $i = 2, 3$)	22 5 5	21.1 \pm 1.2 7.2 \pm 0.7 6.1 \pm 0.6	37
λ'_{ijk} , $i = 1, 2, 3$, $j, k = 1, 2$ $N_{95} = 10.7$ λ'_{i3k} , $i = 1, 2, 3$, $k = 1, 2$, λ'_{ij3} , $i = 1, 2, 3$, $j = 1, 2$ $N_{95} = 4.4$ λ'_{i33} , $i = 2, 3$ $N_{95} = 5.3$				

Table 1: $\tilde{\chi}_1^+$ indirect decay analysis with $\tilde{\chi}_1^0 \rightarrow \nu qq$. The efficiency corresponds to $\tilde{\chi}_1^+ \tilde{\chi}_1^-$ simulated signal with $m_{\tilde{\chi}_1^+} = 70$ GeV / c^2 and $m_{\tilde{\chi}_1^0} = 45$ GeV/ c^2

in the $\tilde{\chi}_1^0$ decay, a two-dimensionnal cut in the plane visible mass vs charged energy and the b-tagging variable $\log_{10}(-\log_{10}(P_E^+))$ since at least one b quark is expected in the $\tilde{\chi}_1^0$ decay. The number of remaining real events and Monte-Carlo events are reported in table 3.

The 95 % confidence level is calculated according the Feldman and Cousins prescription [15]. The content of the Fisher variable in each case is described in table 4. Y_4 and Y_6 are respectively the Durham distance at which the event topology flips from 3 to 4 jets and 5 to 6 jets.

The distributions on of the variable for real events and Monte-Carlo events at the different steps of the analysis are shown on figures 3, 4, 5 for the case $\tilde{\chi}_1^0 \rightarrow \nu_i bb$.

5 Case $\tilde{\chi}_1^0 \rightarrow \mu qq$

There are first very general preselection criteria on the charged multiplicity, the charged energy, the number of leptons and the missing momentum (which should not be large since we expect no missing energy in the process $e^+e^- \rightarrow \tilde{\chi}_1^0 \tilde{\chi}_1^0$ and $\tilde{\chi}_1^0 \rightarrow \mu qq$). The event has to contain at least two standard or tight muons which acolinearity should not be close to 180° (i.e they should not be close). The muons have to be energetic and isolated : a constrain is applied on the product of the energy of the muon multiplied by its isolation angle with respect to the nearest charged particle. Then a two-dimensionnal cut is made in the plane $\log_{10}(Y_5)$ vs $\log_{10}(1 - thrust)$ (Y_5 is the Durham distance at which the event

λ'_{ijk}	Fisher variable	Discriminating power
$i = 1, 2, 3, j = 1, 2, k = 1, 2$	$u = 0.949 \times \log_{10}(Y_6) + 0.0329 \times E_{miss}$ $-1.12 \times (Invisible_{mass}/Visible_{mass})$ $+0.184 \times \log_{10}(\pi - acoplanarity)$	0.473
$i = 1, 2, 3, j = 3, k = 1, 2$ $i = 1, 2, 3, j = 1, 2, k = 3$	$0.505 \times \log_{10}(-\log_{10}(P_E)) + 0.0274 \times E_{miss}$ $+0.734 \times \log_{10}(Y_6)$ $-0.746 \times (Invisible_{mass}/Visible_{mass})$	0.551
$i = 2, 3, j = 3, k = 3$	$0.638 \times \log_{10}(-\log_{10}(P_E)) + 0.755 \times \log_{10}(Y_6)$ $+0.0113 \times E_{miss}$	0.700

Table 2: Content of the Fisher variable for $\tilde{\chi}_1^+$ indirect analysis and the $\tilde{\chi}_1^0$ decay $\tilde{\chi}_1^0 \rightarrow \nu_i q q$

topology flips from 4 to 5 jets). In the case of λ'_{213} and λ'_{223} when a b quark is also present in the $\tilde{\chi}_1^0$ decay the b-tagging variable $\log_{10}(-\log_{10}(P_E^+))$ is used. The number of remaining real events and Monte-Carlo events are reported in table 5.

The 95 % confidence level is calculated according the Feldman and Cousins prescription [15].

6 Results and conclusion

The analyses presented in this paper are covering the pair production of neutralino and chargino with λ'_{2jk} ($j = 1, 2, k = 1, 2, 3$) couplings on one hand and λ'_{i3k} ($i = 1, 2, 3, k = 1, 2, 3$) on the other hand. The common value for the λ' couplings was set to 0.01. No excess of data with respect to the Standard Model expectation has been observed. The results obtained are then used to constrain domains of the MSSM parameter space with the given value of N_{95} ; the different contributions from the different channels in one analysis are added to obtain the total number of expected SUSY signal events, which is compared to the value of N_{95} to derive the limits. Each analysis gives exclusion areas in $\mu - M_2$ planes. The whole exclusion area for one coupling is the union of all the excluded domains of the different analysis designed for this coupling. For each analysis presented in this note, twelve planes have been studied corresponding to the values $\tan\beta = 1.01$, $\tan\beta = 1.5$, $\tan\beta = 5$, $\tan\beta = 30$, $m_0 = 90 \text{ GeV}/c^2$, $m_0 = 300 \text{ GeV}/c^2$ and $m_0 = 500 \text{ GeV}/c^2$. The exclusion plots for λ'_{i3k} ($i = 1, 2, 3, k = 1, 2, 3$) are shown on figures 6, 7. Lower mass limits for the lightest neutralino and the lightest chargino are also obtained. The limit is close to the kinematical limit for $\tilde{\chi}_1^+$ and is a function of $\tan\beta$ for $\tilde{\chi}_1^0$. The corresponding curves are presented on figures 8 for λ'_{2jk} ($j = 1, 2, k = 1, 2, 3$) and λ'_{i3k} ($i = 1, 2, 3, k = 1, 2, 3$) couplings. The results are the following :

- $m(\tilde{\chi}_1^0) \geq 30 \text{ GeV}/c^2$
- $m(\tilde{\chi}_1^+) \geq 94 \text{ GeV}/c^2$

Step	Selection criteria	Data	Background	Efficiency
1	Charged multiplicity ≥ 10 $E_{char} \geq 25$ GeV Invisible Mass ≥ 40 GeV $Pt_{miss} \geq 5$ GeV/c $ \cos(\theta_{miss}) \leq 0.9$	3220	3098 ± 14.2	83
2	$Vis_{mass} \leq 120$ $Vis_{mass} \leq 1.5 \times E_{char} + 10$	1615	1529.0 ± 11.2	64
3	$\log_{10}(-\log_{10}(P_E^+)) \geq -0.2$	685	680.8 ± 7.3	57
4	Fisher Variable $u \geq$ -1.7 ($\lambda'_{i3k}, i = 1, 2, 3, k = 1, 2$) $\lambda'_{ij3}, i = 1, 2, 3, j = 1, 2$ -1.4 ($\lambda'_{i33}, i = 2, 3$)	17	18.7 ± 1.4	22
		6	5.4 ± 0.6	26
$\lambda'_{i3k}, i = 1, 2, 3, k = 1, 2, \lambda'_{ij3}, i = 1, 2, 3, j = 1, 2 N_{95} = 9.0$ $\lambda'_{i33}, i = 2, 3 N_{95} = 7.3$				

Table 3: $\tilde{\chi}_1^0$ direct decay analysis with $\tilde{\chi}_1^0 \rightarrow \nu b q$, $q \neq b$ or $q = b$. The efficiency corresponds to $\tilde{\chi}_1^0 \tilde{\chi}_1^0$ simulated signal with $m_{\tilde{\chi}_1^0} = 60$ GeV/ c^2

References

- [1] Search for Gauginos in R-Parity Violating Scenario with λ' Couplings Involving b-Quarks at $\sqrt{s} = 183$ GeV. C.Mulet-Marquis, DELPHI note 98-171
- [2] For a review see for instance Supersymmetry, supergravity and particle physics H.P.Nilles Phys. Rep. : 110 (1984); The search for supersymmetry : probing physics beyond the standard model H.E. Haber, G.L. Kane, Phys. Rep. : 117(1985)
- [3] An Introduction to Explicit R-Parity Violation. H. Dreiner to be published in Perspectives on Supersymmetry G L Kane World Sci., Singapore hep-ph/9707435; and references therein.
- [4] Lifetime Tag of events $Z^0 \rightarrow b\bar{b}$ with the DELPHI detector AABTAG program. G.Borisov. DELPHI 94-125 PROG 208, 11, August 1994.
- [5] Combined b-Tagging. G.Borisov. DAPNIA/SPP 97-28, November 1997.
- [6] Dominance of Pion Exchange in R-Parity Violating Supersymmetric Contributions to Neutrinoless Double Beta Decay. A. Fässler, S.Kovalenko, F.Šimkovic, J.Schwieger; Phys.Rev.Lett volume 78, numéro 2 (1997), 183-186.
- [7] Indirect limits on SUSY Rp violating couplings λ and λ' . F.Ledroit, G.Sajot GDR-S-008
http://qcd.th.u-psud.fr/GDR_SUSY/GDR_SUSY_PUBLIC/entete_note_publicue
- [8] Pythia: the Lund Monte-Carlo for Hadronics processes. H.U. Bengtsson, T.Sjöstrand; Computer Physics Communications 39(1986) 347.

λ'_{ijk}	Fisher variable	Discriminating power
$i = 1, 2, 3, j = 3, k = 1, 2$ $i = 1, 2, 3, j = 1, 2, k = 3$	$0.774 \times \log_{10}(-\log_{10}(P_E^+)) + 0.479 \times \log_{10}(Y_4)$ $+0.393 \times \log_{10}(\pi - \text{acoplanarity})$ $+0.516 \times \log_{10}(Y_6) - 0.641 \times \log_{10}(1 - \text{thrust})$	0.405
$i = 2, 3, j = 3, k = 3$	$1.09 \times \log_{10}(-\log_{10}(P_E^+)) + 0.724 \times \log_{10}(Y_6)$ $+0.201 \times \log_{10}(\pi - \text{acoplanarity})$ $-0.456 \times \cos(\theta_{\text{miss}}) $	0.550

Table 4: Content of the Fisher variable $\tilde{\chi}_1^0$ direct decay analysis with $\tilde{\chi}_1^0 \rightarrow \nu bq$, $q \neq b$ or $q = b$

Step	Selection criteria	Data	Background	Efficiency
1	Charged multiplicity ≥ 10 $E_{\text{char}} \geq 35$ GeV At least one lepton $P_{\text{miss}} \leq 40$ GeV/c	4425	4490 ± 15.3	85
2	At least 2 standard muons Acolinearity of muons $\leq 150^\circ$	62	62.8 ± 2.0	48
3	$\log_{10}(E_{\mu 1} \times \theta_{\text{isol}1}) \geq 2$ $\log_{10}(E_{\mu 2} \times \theta_{\text{isol}2}) \geq 1.6$	8	9.7 ± 0.7	42
4	$\log_{10}(Y_5) \geq$ $-2.25 + \log_{10}((1 - \text{thrust}))$	1	4.3 ± 0.5	40
Case of λ'_{213} and λ'_{223} couplings				
5	$\log_{10}(-\log_{10}(P_E^+)) \geq 0$	0	1.9 ± 0.3	32

Table 5: $\tilde{\chi}_1^0$ direct decay analysis with $\tilde{\chi}_1^0 \rightarrow \mu qq$, The efficiency corresponds to $\tilde{\chi}_1^0 \tilde{\chi}_1^0$ simulated signal with $m_{\tilde{\chi}_1^0} = 40$ GeV/ c^2 . The b-tagging variable $\log_{10}(-\log_{10}(P_E^+))$ is used only for λ'_{213} and λ'_{223} when a b quark is present

- [9] The Monte-Carlo Program Koralz, Version 4.0, for the Lepton or Quark Pair Production at LEP / SLC Energies. S. Jadach, B.F.L Ward and Z. Was; Computer Physics Communications 79(1994) 503
- [10] Monte-Carlo Simulation of two Photons Processes. F.A. Berends, P.H. Davervelt, R. Kleiss; Computer Physics Communications 40 (1986) 271
- [11] S. Nova, A. Olchevski, T. Todorov, Delphi 90-35 PROG 512
- [12] Excalibur: a Monte-Carlo Program to Evaluate all Four Fermion Processes at LEP-200 and Beyond. F.A. Berends, R. Pittau, R. Kleiss Computer Physics Communications 85 (1995) 437.

- [13] SUSYGEN 2.2: a Monte-Carlo Event Generator for MSSM Sparticle Production at e^+e^- colliders. S. Katsanevas P. Morawitz; Computer Physics Communications 112 (1998) 227.
- [14] The advanced Theory of Statistics, vol 3, third edition 1976, ed. Charles Griffin and co; M.Kendall, A.Stuart.
Un Exemple d'analyse multidimensionnelle : l'analyse discriminante; P.Lutz. Gif 88, Ecole d'été de physique nucléaires et de physique des particules; 12-16 september 1988.
- [15] Unified Approach to the Classical Statistical Analysis of Small Signals. G.J.Feldman, R.D.Cousins; Phys.Rev D 57, no 7 (1998), 3873-3889.

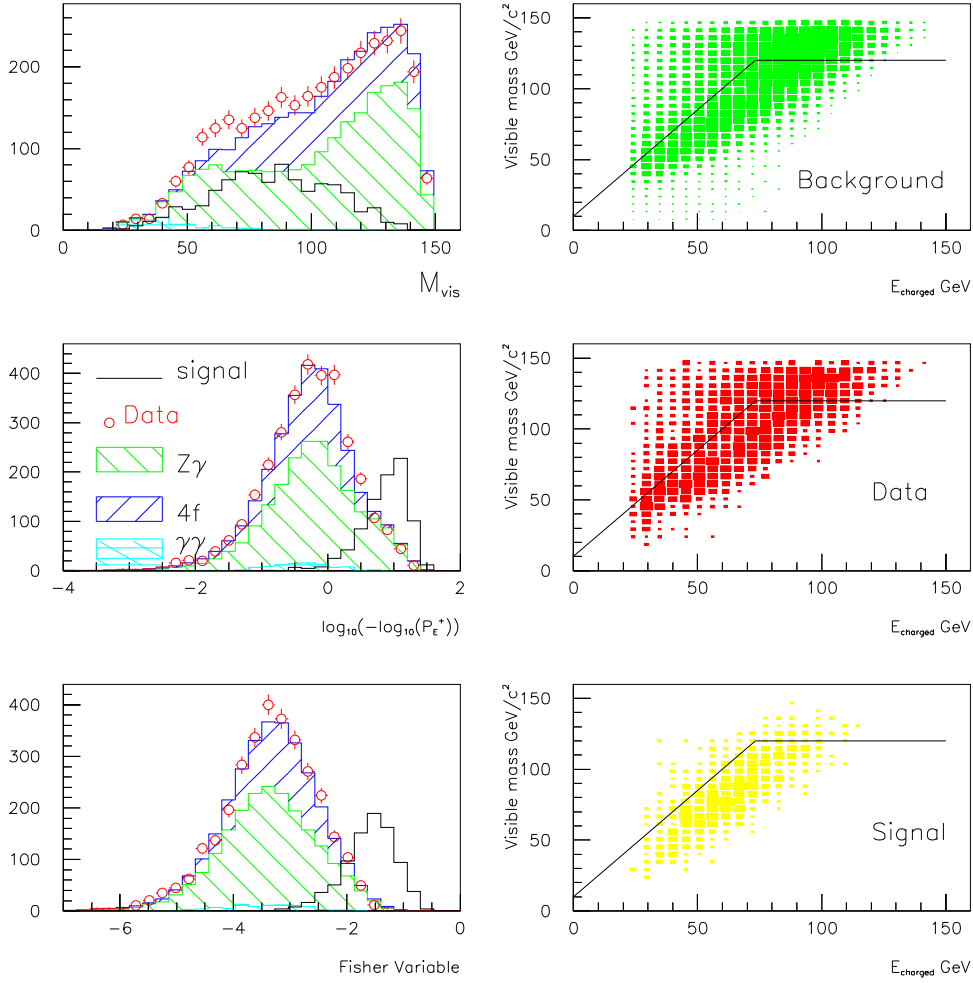


Figure 3: Distribution of the event variables for $e^+e^- \rightarrow \tilde{\chi}_1^0 \tilde{\chi}_1^0$ and $\tilde{\chi}_1^0 \rightarrow \nu b b$ analysis at the step 1 level of table 3 for data (dots), expected SM background (hatched histograms) and signal (full line histograms).

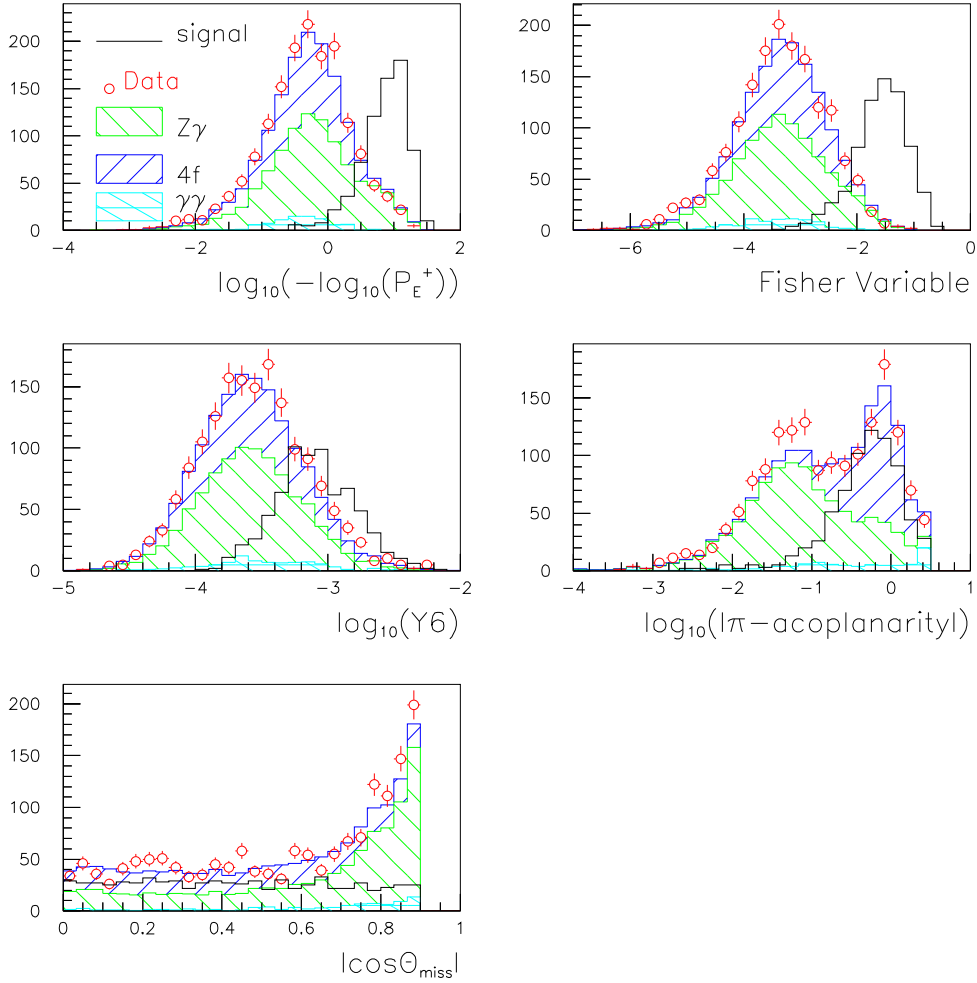


Figure 4: Distribution of the event variables for $e^+e^- \rightarrow \tilde{\chi}_1^0\tilde{\chi}_1^0$ and $\tilde{\chi}_1^0 \rightarrow \nu bb$ analysis at the step 2 level of table 3 for data (dots), expected SM background (hatched histograms) and signal (full line histograms).

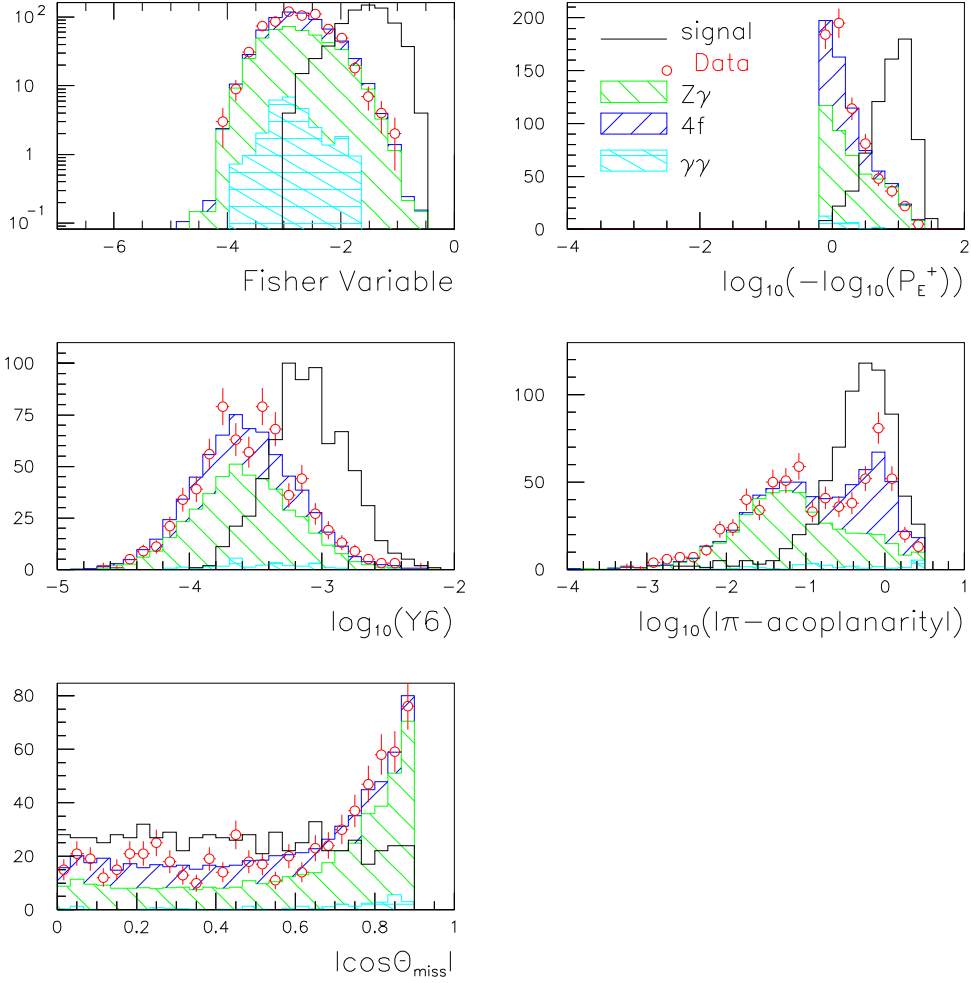


Figure 5: Distribution of the event variables for $e^+e^- \rightarrow \tilde{\chi}_1^0 \tilde{\chi}_1^0$ and $\tilde{\chi}_1^0 \rightarrow \nu bb$ analysis at the step 3 level of table 3 for data (dots), expected SM background (hatched histograms) and signal (full line histograms). $\log_{10}(-\log_{10}(P_E^+))$, $\log_{10}(Y_6)$, $\log_{10}(|\pi - \text{acoplanarity}|)$ and $|\cos(\theta_{\text{miss}})|$ are the four variable used in the Fisher analysis

DELPHI Preliminary

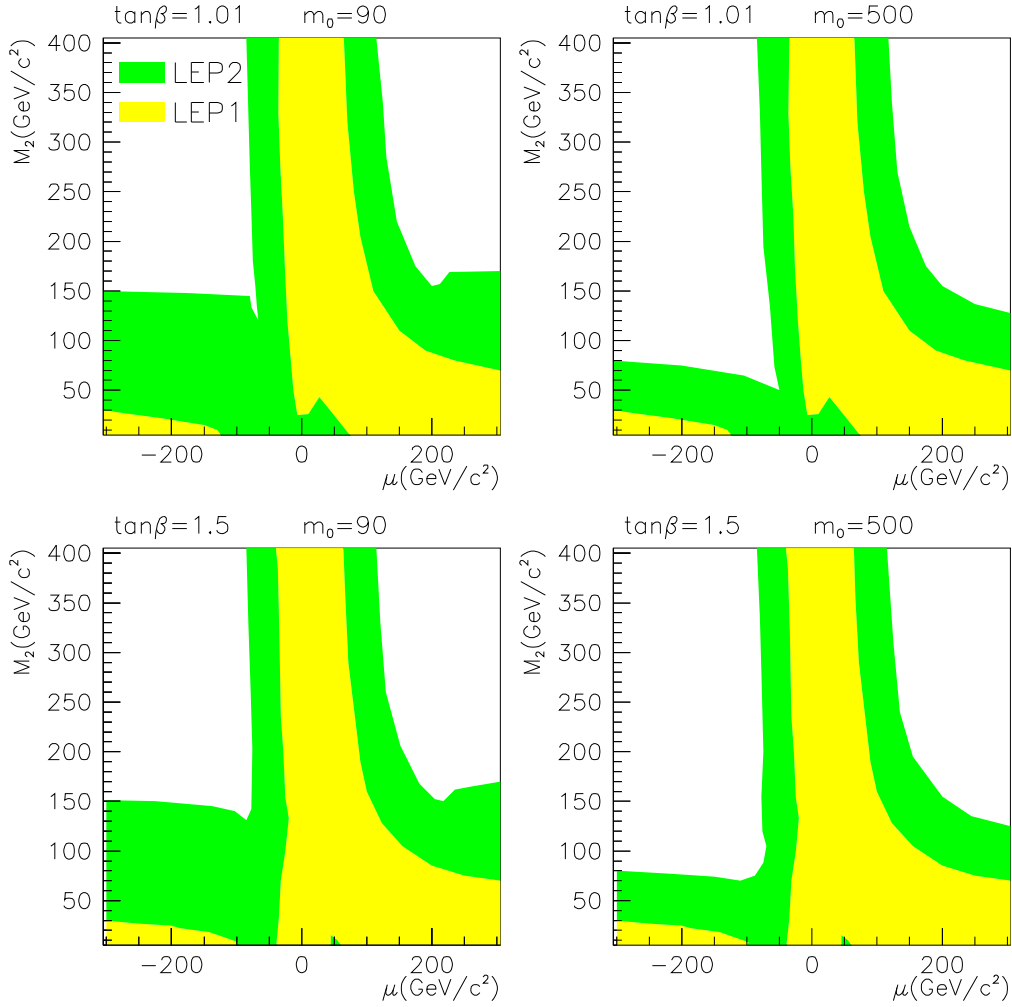


Figure 6: Exclusion area at 95 % CL for λ'_{i3k} ($i = 1, 3$, $k = 1, 2, 3$) dominant couplings (with the value $\lambda'_{i3k} = 0.01$) in four $\mu - M_2$ planes ($\tan\beta = 1.01$, $\tan\beta = 1.5$, $m_0 = 90$ GeV/c² and $m_0 = 500$ GeV/c²). The light grey regions (or yellow in colour) are excluded by LEP1 results, the dark grey (or green in colour) are those excluded by the present analysis.

DELPHI Preliminary

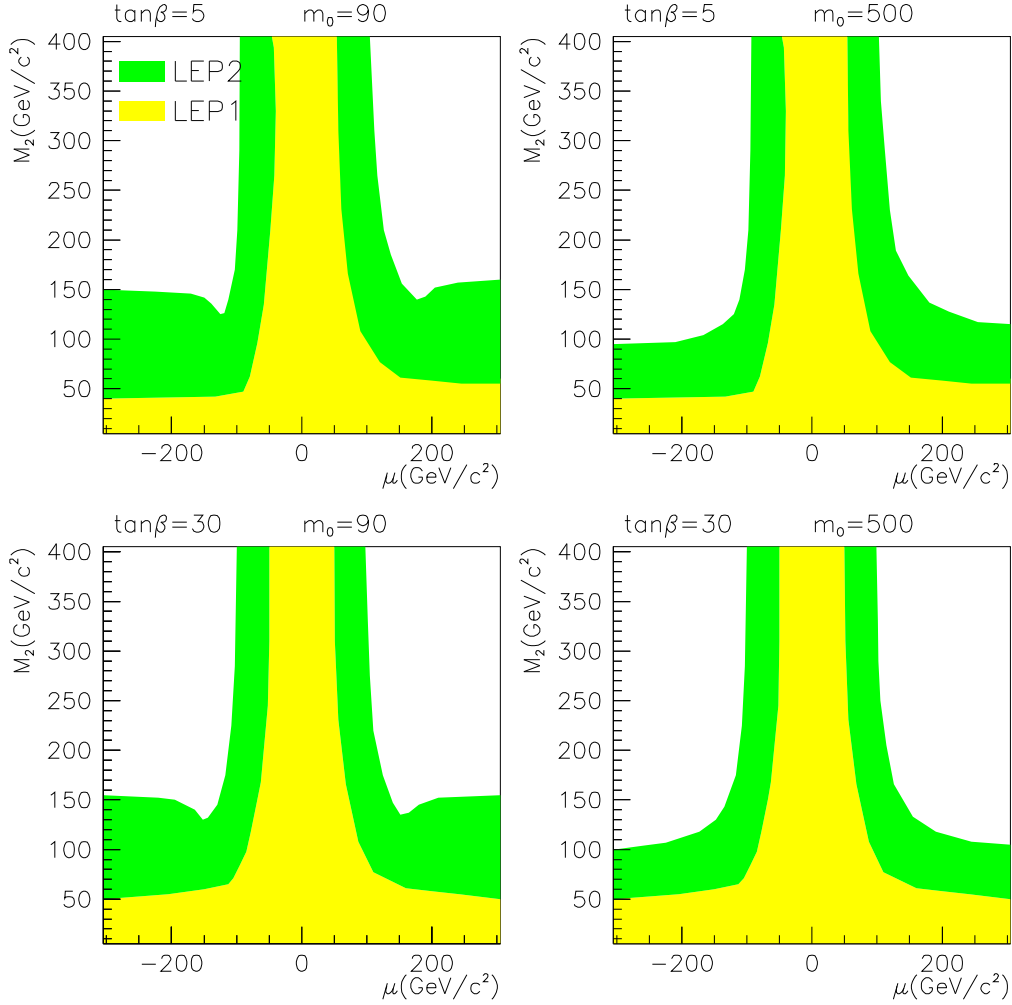


Figure 7: Exclusion area at 95 % CL for λ'_{i3k} ($i = 1, 3, k = 1, 2, 3$) dominant couplings (with the value $\lambda'_{i3k} = 0.01$) in four $\mu - M_2$ planes ($\tan\beta = 5, \tan\beta = 30, m_0 = 90 \text{ GeV}/c^2$ and $m_0 = 500 \text{ GeV}/c^2$). The light grey regions (or yellow in colour) are excluded by LEP1 results, the dark grey (or green in colour) are those excluded by the present analysis.

DELPHI Preliminary

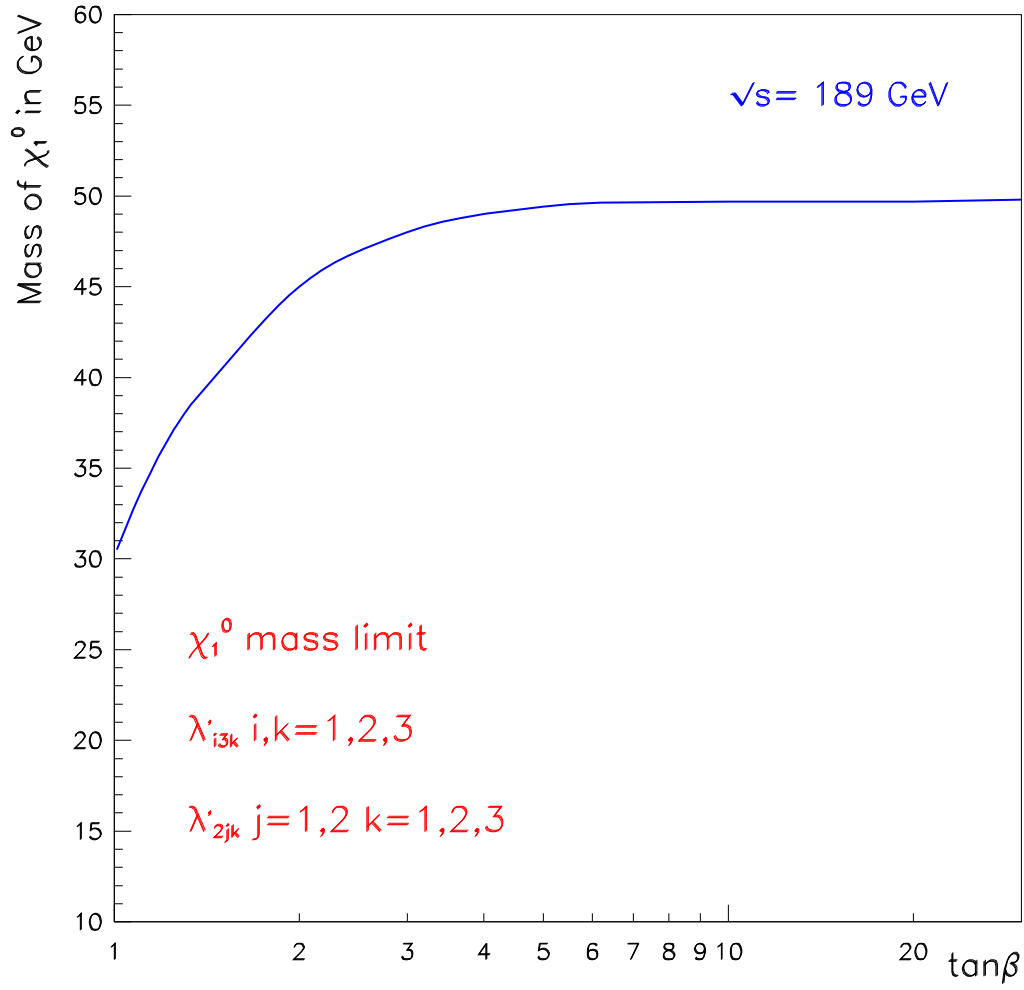


Figure 8: Lower limit on the $\tilde{\chi}_1^0$ mass as a function of $\tan\beta$ for λ'_{i3k} ($i = 1, 3, k = 1, 2, 3$) and λ'_{2jk} ($j = 1, 2, k = 1, 2, 3$) couplings (with a common value of 0.01 for the λ' couplings).